Published in final edited form as:
Hum Mutat. 2007 March ; 28(3): 243–254. doi:10.1002/humu.20425.

Transgenic Mice Carrying the *H258N* Mutation in the Gene Encoding the β-Subunit of Phosphodiesterase-6 (PDE6B) Provide a Model for Human Congenital Stationary Night Blindness

Stephen H. Tsang[1,*], **Michael L. Woodruff**[2], **Lin Jun**[1], **Vinit Mahajan**[3], **Clyde K. Yamashita**[2], **Robert Pedersen**[5], **Chyuan-Sheng Lin**[1], **Stephen P. Goff**[7], **Thomas Rosenberg**[6], **Michael Larsen**[5,6], **Debora B. Farber**[2,4], and **Steven Nusinowitz**[2]

[1] Brown Glaucoma Laboratory, Center for Neurobiology and Behavior, Columbia University, New York, New York

[2] Jules Stein Eye Institute, University of California, Los Angeles (UCLA), Los Angeles, California

[3] Omics Laboratory, Jules Stein Eye Institute, UCLA, Los Angeles, California

[4] Molecular Biology Institute, UCLA, Los Angeles, California

[5] Glostrup Hospital, University of Copenhagen, Copenhagen, Denmark

[6] Gordon Norrie Centre for Genetic Eye Diseases, National Eye Clinic for the Visually Impaired, Hellerup, Denmark

[7] Howard Hughes Medical Institute, Department of Biochemistry and Molecular Biophysics, Columbia University, New York, New York

Abstract

Mutations in the β-subunit of cGMP-phosphodiesterase (PDE6β) can lead to either progressive retinal disease, such as human retinitis pigmentosa (RP), or stationary disease, such as congenital stationary night blindness (CSNB). Individuals with CSNB in the Rambusch pedigree were found to carry the *H258N* allele of *PDE6B* (MIM# 180072); a similar mutation was not found in RP patients. This report describes an individual carrying the *H258N* allele, who presented with generalized retinal dysfunction affecting the rod system and a locus of dysfunction at the rod-bipolar interface. Also described are preclinical studies in which transgenic mice with the *H258N* allele were generated to study the pathophysiological mechanisms of CSNB. While $Pde6b^{rd1}/Pde6b^{rd1}$ mice have severe photoreceptor degeneration, as in human RP, the *H258N* transgene rescued these cells. The cGMP-PDE6 activity of dark-adapted *H258N* mice showed an approximate three-fold increase in the rate of retinal cGMP hydrolysis: from 130.1 nmol × min^{-1} × $nmol^{-1}$ rhodopsin in wild-type controls to 319.2 nmol × min^{-1} × $nmol^{-1}$ rhodopsin in mutants, consistent with the hypothesis that inhibition of the PDE6β activity by the regulatory PDE6γ subunit is blocked by this mutation. In the albino (B6CBA × FVB) F2 hybrid background, electroretinograms (ERG) from *H258N* mice were similar to those obtained from affected Rambusch family members, as well as humans with the most common form of CSNB (X-linked), demonstrating a selective loss of the *b*-wave with relatively normal *a*-waves. When the *H258N* allele was introduced into the DBA background, there was no evidence of selective reduction in *b*-wave amplitudes; rather *a*- and *b*-wave amplitudes were both reduced. Thus, factors other than the *PDE6B* mutation itself could contribute to the variance of an

*Correspondence to: Stephen H. Tsang, MD, PhD, Brown Glaucoma Laboratory, Center for Neurobiology and Behavior, Columbia University, New York, New York. E-mail: sht2@columbia.edu.

Communicated by Peter Humphries

electrophysiological response. Therefore, caution is advisable when interpreting physiological phenotypes associated with the same allele on different genetic backgrounds. Nevertheless, such animals should be of considerable value in further studies of the molecular pathology of CSNB.

Keywords

congenital stationary night blindness; retinal dystrophy; animal model; PDE6

INTRODUCTION

Many neurotransmitters and hormones signal target cells through G-protein-coupled receptors. Light acts similarly in the retinal photoreceptor cells, thereby initiating a signal transduction cascade that results in hyperpolarization of the photoreceptor plasma membrane. In rods, rhodopsin, a G-protein-coupled receptor, transduces the light signal. Upon absorption of a photon, rhodopsin becomes photoexcited and activates the α-subunit of G-protein transducin (GNAT1), which in turn binds its effector, the phosphodiesterase-6 γ (PDE6γ) subunit [Arshavsky et al., 2002; Baehr et al., 1979; Burns and Arshavsky, 2005; Burns and Baylor, 2001; Fain et al., 2001; Fung et al., 1981, 1990; Stryer, 1991; Tsang and Gouras, 1999; Tsang et al., 1996; Yarfitz and Hurley, 1994; Zhang and Cote, 2005; Guo et al., 2005], and relieves PDE6γ's inhibition of the PDE6αβ catalytic subunits [Guo et al., 2006]. Activated PDE6αβ then lowers cytoplasmic cyclic guanosine 3′, 5′-monophosphate (cGMP) concentrations, thereby closing cGMP-gated cationic channels in the rod plasma membrane and generating a change in membrane current that can be recorded in real time [Baylor et al., 1979]. During recovery from the photoresponse, GNAT1 is deactivated by hydrolysis of bound GTP [Slep et al., 2001], permitting PDE6γ to rapidly reinhibit PDE6αβ.

Photoreceptors generally have two ways of reacting to genetic insults: "self-destruction" or "dysfunction," manifested as retinitis pigmentosa (RP) or congenital stationary night blindness (CSNB), respectively [Lem and Fain, 2004]. Night blindness, resulting from progressive degeneration of rod photoreceptors, is an early symptom of RP. Later, tunnel vision and loss of central vision develop as cones degenerate. Individuals with CSNB, on the other hand, do not exhibit photoreceptor cell death, but show signs of rod dysfunction. CSNB is a nonprogressive retinal disorder characterized by impaired night vision, decreased visual acuity, myopia, nystagmus, and strabismus. The largest known pedigree in human genetics is one affected by CSNB, who were all descendants of Jean Nougaret [Dryja et al., 1996; Sandberg et al., 1998]. The G38D allele in the rod-specific *GNAT1* gene (MIM# 139330) is responsible for the autosomal dominant form of night blindness [Dryja et al., 1996; Sandberg et al., 1998]. Although every affected Nougaret family member was heterozygous at the *GNAT1* locus [Dryja et al., 1996; Sandberg et al., 1998], in mice, reduced rod photoreceptor responses were found only in homozygous *Tg*(*Gnat1G38D*)*; Gnat1*^{tm1Clma}*Gnat1*^{tm1Clma}, but not heterozygous *Tg*(*Gnat1G38D*)*; Gnat1*^{tm1Clma}*Gnat1*^{tm1Clma}/+ mice [Moussaif et al., 2006].

Why abnormalities in a rod-specific protein, PDE6β (MIM# 180072) cause nonprogressive CSNB [Gal et al., 1994] in some cases and progressive rod-cone degeneration in others [Danciger et al., 1995; McLaughlin et al., 1993, 1995] is not known. *PDE6B* gene defects were ultimately demonstrated to be the most commonly identified cause of autosomal recessive RP, accounting for 4 to 5% of cases [McLaughlin et al., 1995; Danciger et al., 1995].

A base change in exon 4 that causes a neutral, hydrophilic asparagine (N) to be encoded in place of a basic, hydrophilic histidine (H) in *PDE6B* was found to be associated with CSNB in the Sorensen family, first described by Rambusch in 1909 [Gal et al., 1994; Rosenberg et al., 1991]. The Rambusch pedigree consisted of 200 affected individuals over 11 generations.

Affected individuals achieved 20/20 vision, but had dark adaptation thresholds elevated by 2.5 to 3.0 logarithmic units [Rosenberg et al., 1991], Under dark-adapted conditions, some affected individuals in the Rambusch family demonstrated reduced *b*-wave amplitudes but relatively normal *a*-waves [Rosenberg et al., 1991]; this study concluded that "the *b*-wave exhibited pronounced reduction in amplitude" [Rosenberg et al., 1991], The light-adapted cone 32-Hz white flickering responses obtained from these individuals were described as having "normal or slightly reduced amplitudes and normal implicit times"; the maximal dark-adapted electroretinogram (ERG) responses were mildly electronegative (i.e., a reduced *b*- to *a*-wave amplitude ratio) with a normal *a*-wave confirming normal photoreceptor function, but a reduced *b*-wave in the maximal response.

The *H258N* missense mutation associated with CSNB has not been found in RP patients [Gal et al., 1994]; this mutation, in PDE6β, is located in the conserved noncatalytic cGMP-binding regulatory module found in cGMP-regulated PDE, adenyl cyclases, and the *E. coli* protein FhlA (GAP). Each PDE6β subunit contains an N-terminal domain of unknown function, tandem GAP domains (GAFa and GAFb) and a C-terminal catalytic domain. The GAP domain is where PDE6γ exerts its control [Guo et al., 2005], The noncatalytic GAFa domain is distinct from the cGMP hydrolytic site, but also binds cGMP with high affinity. In the dark-adapted rod, intracellular cGMP (60 μM total) is present in two pools: free [2 μM] and is mostly bound to GAF domains on PDE6 [Mou et al., 1999; Muradov et al., 2003; Zhang and Cote, 2005]. The cGMP content of photoreceptor rod outer segments (ROS) only drops to 50% during prolonged light exposure [Woodruff and Bownds, 1979]. The physiological role of PDE6-bound cGMP remains uncertain [Zhang and Cote, 2005].

While the function of the GAFb domain is not known, GAFa controls the specificity [Zoraghi et al., 2004] of PDE dimerization. In contrast to GAF domains in PDE2 or PDE5, the GAF domains in PDE6 are uncoupled from the catalytic sites [Zoraghi et al., 2004]. Binding of cGMP to the GAFa domain increases the affinity between PDE6γ and the catalytic domain, leading to a decrease in cGMP hydrolysis [Mou and Cote, 2001]. PDE6γ dissociates from the PDE6β catalytic core only when cGMP dissociates from the GAF domains of PDE6β [D'Amours and cote, 1999; Norton et al., 2000]. The central region (amino acid residues 20–40) of PDE6γ stimulates cGMP binding to the GAFa domain of PDE6αβ in a reciprocal manner [Arshavsky et al., 1992; Cote, 2000; Yamazaki et al., 2002]. Thus, there is positive cooperativity between PDE6γ and cGMP binding to GAFa.

To study the effects of *H258N* in cultured Sf9 insect cells [Muradov et al., 2003], the authors used a PDE6α′/PDE5 chimera carrying H257N as a model system. Although this H257N mutant can bind cGMP directly, there is a 20-fold decrease in binding of PDE6γ. Impaired PDE6γ inactivation of *H258N* should constitutively stimulate PDE6β and desensitize the rods as seen in the Rambusch family. To test this hypothesis in vivo, we generated transgenic mice carrying the H258N allele.

Initially, the *H258N* allele was analyzed in the (B6CBA × FVB) F2 mixed background. Subsequently, studies were conducted in the DBA inbred background. The DBA inbred strain, developed by C.C. Little, is the oldest of all inbred strains of mice [Bailey, 1978], and is commonly used with the B6 strain to generate oocytes (B6D2) for transgenic experiments [Chen et al., 1996; Wakayama et al., 2005]. Although aged DBA mice develop pigmentary glaucoma, retinal function is normal for at least the first 6 months of their life [Bayer et al., 2001; Piccolino et al., 1989; Schuettauf et al., 2004].

MATERIALS AND METHODS

Human Electrophysiological Testing

Full-field ERGs to test retinal function were performed using extended testing protocols incorporating the International Society for Clinical Electrophysiology of Vision (ISCEV) standard [Marmor et al., 2003], The minimum protocol incorporates the rod-specific and standard bright flash ERGs, both recorded after a minimum of 20 minutes dark adaptation. Following 10 minutes of light adaptation, the photopic 30-Hz flicker cone and transient photopic cone ERGs were recorded. A stimulus 0.6 log units greater than the ISCEV standard flash was also used to better demonstrate the *a*-wave, as suggested in the recent revision of the ISCEV standard for ERG [Marmor et al., 2003]. Pupils were dilated before full-field ERG testing using tropicamide (1%) and phenylephrine hydrochloride (2.5%).

Human Genetic Analyses

DNA was extracted from the blood of an individual with CSNB. Extracted genomic DNA was amplified for sequencing in 30-μl PCR reactions using standard methodology.

Generation of Mutant Mouse Lines

Mice were used in these experiments in accordance with the Association for Research and Vision in Ophthalmology statement for the Use of Animals in Ophthalmic and Vision Research. DNA constructs for the expression of PDE6β contained 4.4 kilobase (kb) of the mouse opsin promoter, the complete open reading frame of the *Pde6b* cDNA, and the polyadenylation signal of the mouse protamine gene [Lem et al., 1991]. The *H258N* point mutation was introduced by a standard PCR-based site-specific mutagenesis strategy [Tsang et al., 1998]. The entire *Pde6b* cDNA coding region in the latter construct was sequenced to confirm introduction of the point mutation and no other inadvertent changes. Vector sequences were excised using Kpnl and Xbal.

Oocytes were obtained from superovulated B6CBAF1 females mated with B6CBAF1 males. Control and *H258N* constructs were injected into the male pronuclei of oocytes under a depression slide chamber. These microinjected oocytes were cultured overnight in M16 (Specialty Media, Phillipsburg, NJ) and transferred into the oviducts of 0.5-day postcoitum pseudopregnant B6CBAF1 females. The resulting transgenic mice were then backcrossed, initially into the FVB background, and subsequently with DBA mice to place the transgene into the *Pde6brd1/Pde6brd1* background.

The first examinations were conducted in the albino (B6CBA × FVB) F2 mixed genetic background. However, subsequent studies were conducted in the inbred DBA strain. N10 from such crosses were used for the subsequent physiological assays. The pigmented N10 mice were also tested for the presence of the *Pde6brd1* allele [Pittler and Baehr, 1991].

Identification of Transgenic Mice

DNA was isolated from tail tips or liver samples by homogenizing the tissue, digesting extensively with proteinase K, and extracting with phenol. DNA was analyzed by PCR and by Southern blot hybridization with a *Pde6b* probe. Additional restriction digests were performed to determine the structure of the integrated sequences and to insure that the DNA flanking the transgene was intact.

Extracted genomic DNA was amplified for sequencing in 30-μl PCR reactions using standard methodology. Nested PCR and primer-specified restriction map modification [Sorscher and Huang, 1991] were used for subsequent genotyping of the *H258N* allele in transgenic mouse tail DNA. PCR amplification of exon 4 resulted in a 620-bp fragment using the forward primer

< 5′ gaagatgataaacgtgcaggatg > and the reverse primer < 5′ taaagccactttctgctacgtagg>. The C to A transversion in the *H258N* allele could be detected specifically in a subsequent round of reamplification of the 620-bp product using a mutant primer <5′ aggtgtttgaagagctgacagacatcgaaagacagGtc > to introduce a T to G mismatch in codon 257; this, in conjunction with the *H258N* allele, yielded a new HincII restriction site. This mutant forward primer was used with another reverse primer < 5′ ggaggatataatcgatgactttgtagaag> to generate 260-bp and 80-bp fragments after HincII digestion of the reamplified PCR product. The *Pde6brd1* allele, which did not contain any HincII restriction site, yielded a 340-bp product in this nested amplification.

Isolation of ROSs

Under dim red light conditions, ROSs from dark-adapted mice were isolated in HEPES/phosphate balanced salt solution (4.09 mM sodium phosphate monobasic, 14.7mM HEPES-pH 7.2, 148.4mM NaCl, 4.91 mM KCl, 2.45mM $CaCl_2$, and 1.23mM $MgSO_4$). Rhodopsin content was determined by the difference in absorbance at 500 nm before and after bleaching under a nonsaturating halogen light source [Zimmerman and Godchaux, 1982].

Immunoblot Analyses

Proteins from murine ROSs (185 pmol rhodopsin/lane) were separated by electrophoresis on either a 6.5% to 9.5% acrylamide/1.5% crosslinker (for PDE6α and β subunits) or a 12% acrylamide/1.5% crosslinker (for the PDE6γ subunit) inverted gradient polyacrylamide gel, previously described by Tsang et al. [1996]. Proteins were then transferred to 0.2 μm PVDF membranes (BioRad Laboratories, Hercules, CA) overnight at 4 V/cm [Towbin et al., 1979]. Membranes were blocked in 3% bovine serum albumin (BSA) in 500mM NaCl, 20mM Tris, pH 7.6, and 0.1% Tween 20. PDE6α and β subunits were detected with a polyclonal antiserum raised against a 17-mer peptide [Piriev et al., 1993; Tsang et al., 2006] that is 100% homologous between the rod PDE6α and β subunits as well as the cone PDEα′ subunit. Western blots were visualized with the DuoLux Chemiluminescence substrate kit (Vector Laboratories, Inc., Burlingame, CA) utilizing a goat anti-rabbit IgG-alkaline phosphatase conjugate. Blots were exposed to Hyperfilm-MP (Amersham Pharmacia Biotech, Piscataway, NJ) and preflashed to increase sensitivity and linearity according to the Sensitize™ protocol (Amersham Pharmacia Biotech). Signals were quantified by densitometric scanning.

PDE Activity Assay

To measure both dark- (basal) and light-stimulated PDE6 activities, animals were dark-adapted overnight and then retinas were dissected under far red light (Kodak Type 11 filter). Retinas were incubated for 10 minutes in hypotonic buffer supplemented with 1 mM ATP [Bitensky et al., 1975; Kamps and Hofmann, 1986] and 5μM GTPγS [Wensel and Stryer, 1986]; then, for 2 extra minutes, they were either maintained in the dark or exposed to room light. Retinas were then homogenized, centrifuged for 10 minutes at 8,000 g and supernatants collected. Aliquots were removed for protein determination by the method of Peterson [1977], using BSA as standard. The method of Farber and Lolley [1976] was used to measure cGMP-PDE activity, using 250 μM cGMP as substrate 3 to 10 μg of retinal protein (depending on the sample) were incubated for 15 minutes at 37 °C with the substrate in 40 mM Tris buffer, neutral pH, containing 200,000 cpm 3H-cGMP, 5 mM $MgCl_2$, and 1 mM dithiothreitol (DTT). The reaction was terminated by heating to 80 °C for 3 minutes. Calf intestinal alkaline phosphatase (0.4 U) was then added and incubation continued for 10 minutes at 37°C. The resulting 3H-guanosine was separated from other nucleotides by a resin slurry (AG1-X2, 50–100 mesh; BioRad Laboratories) and radioactivity quantified in a scintillation counter. Results were expressed as nmol of hydrolyzed cGMP × min^{-1} × $nmol^{-1}$ of rhodopsin. To minimize differences between

mice, ROSs of two or more mice were pooled for each time point assayed, and each reaction was carried out in triplicate.

Histology

Mice were euthanized with an intraperitoneal injection of nembutal Each eye was rapidly removed, punctured at the 12 o'clock position along the limbus, and placed in a separate solution of 3% glutaraldehyde in phosphate buffered saline. After fixation for 1–2 days, the eyes were washed with saline and the 12 o'clock limbal puncture was used to orient the right and left eyes, which were kept in separate buffer, so that the posterior segment containing the retina could be sectioned along the vertical meridian. A rectangular piece containing the entire retina from superior to inferior ora serrata, including the optic nerve, was prepared for postfixing in osmic acid, dehydration, and epon embedding. A corner was cut out at the superior ora to identify the upper retinal half of the segment. Sectioning proceeded along the long axis of the segment so that each section contained upper and lower retina as well as posterior pole. Semiserial sections were stained with either hemotoxylin-eosin or toluidine blue, mounted, and examined by light microscopy. Selected areas were trimmed for ultrathin sectioning, stained with uranyl acetate, and examined by electron microscopy.

Mouse ERG

Following overnight dark adaptation, mice were anesthetized by intraperitoneal injection of 15 μg/g ketamine and 7 μg/g xylazine. ERGs were recorded from the corneal surface of the right eye after pupil dilation (1% atropine sulfate) using a gold loop corneal electrode together with a mouth reference and tail ground electrode. Stimuli were produced with a Grass Photic Stimulator (PS33 Plus; Grass Instruments, Quincy, MA) affixed to the outside of a highly reflective Ganzfeld dome. Dark-adapted ERGs were recorded to short-wavelength (Kodak Wratten 47A; I_{max} = 470 nm) flashes of light over a range of intensities up to the maximum allowable by the Grass Photic Stimulator. These responses were fitted with a Naka-Rushton function to estimate V_{max}, the maximum saturated *b*-wave amplitude, and *k*, the semisaturation intensity. The range of stimulus intensities was extended by replacing the Grass flash head with a xenon gas flash tube (Novatron, Inc., Dallas, TX) driven by a 1,600-W power supply. With the Novatron flash head, dark-adapted ERGs were recorded to short-wavelength (Kodak Wratten 47B, Eastman Kodak, Hamden, CT; I_{max} = 450 nm) light flashes up to the maximum intensity of 3.32 log scotopic trolands/s. At the highest stimulus intensities, the leading edge of the *a*-wave of the ERG was fitted with a computational model to provide estimates of photoreceptor activity, generating two parameters, *S*, a sensitivity (or gain) parameter that scales flash energy, and Rm_{P3}, the maximum saturated photovoltage. ERGs under rod-saturating conditions (background of 43.3 cd/m^2) were recorded to white flashes of light up to 4.35 cd/m^2. Response signals were amplified (CP511 AC amplifier; Grass Instruments), digitized (PCI-1200; National Instruments, Austin, TX) and computer-analyzed. Up to 100 recordings were averaged for the weakest signals.

Suction Electrode Measurements

Standard procedures [Woodruff et al., 2003] were used for recording photocurrents from mouse rods using polished, silanized suction pipettes of 0.2–0.3 Mω. Freshly dissected retinas from dark-adapted transgenic and control mice were taped down onto sylgard-coated dishes and chopped with a fine razor. Retinal pieces were transferred with a pipette to an inverted microscope stage, and used to produce isolated rods, rods in small clusters of cells and rods in intact pieces of retina—all of which were then available for suction recording analysis. The samples were superfused with physiological solution containing amino acids and nutrients at 37°C. Stimuli were from halogen lamps (500 nm), with attenuation provided by calibrated absorptive neutral density filters. Current responses were amplified by a Warner Patch Clamp

(Warner Instruments, Rochester, NY) (PC-501A) amplifier and recorded directly into a microcomputer using Pclamp hardware and software (Axon Instruments, Foster City, CA).

Light sensitivity for a given rod was determined using 20 msec stimuli with six (bright flashes) to 20 (dim flashes) responses, averaged to obtain a mean response for that intensity. Intensities from threshold to saturation were presented in 0.5 log unit steps. Dark-adapted flash sensitivity was defined as the intensity at which a just-detectable response is obtained. Incremental flash sensitivities were obtained by making the same determination in the presence of steady background illuminations of various intensities. Single-photon analysis used Poisson statistics as described [Baylor et al., 1979]. Briefly, 20 to 100 dim flash responses were averaged, and the mean squared response was scaled so that its rising phase corresponds to the rising phase of the time-dependent response variance. The scaling factor, the reciprocal of the average number of photoisomerizations generating the mean response, was used to adjust the mean response to the single-photon level.

RESULTS

Genetic Studies

To address how the *H258N* mutation in the *PDE6B* gene affected visual function, we phenotyped one human patient and transgenic mice carrying this allele. The patient was a 36-year-old man with a long history of night blindness. His father, paternal grandfather, paternal great-grandmother, as well as 8 out of 11 children from his grandfather have similar complaints. By history, a paternal uncle was diagnosed with “typical RP.” His diseased father had “tunnel vision.”

On examination, our patient was myopic with manifest refraction: −4.00+3.00 × 005 (right eye) and −4.25+3.00 × 175 (left eye). His visual acuity was 20/20 in the right eye and 20/15 in the left eye (normal = 20/20). His axial length was 22.49 mm and 22.80 mm in the right and left eyes, respectively. No gross abnormality was noted in his fundus examination (reviewed but not shown) Humphrey 10–2 visual fields were full. His past medical history was significant only for a 9-year history of type-1 diabetes.

In 1995, full-field ERGs were performed with Ganzfeld stimulation on this patient. There was generalized retinal dysfunction, with sparing of the cone system (photopic single-flash and 30-Hz flicker ERGs were relatively normal) (Fig. 1). The maximal ERG mixed rod-cone responses induced with maximal stimulus had normal *a*-waves but were electronegative with selective reduction in *b*-wave amplitude (Fig. 1). There have been no significant deviations from the amplitudes and implicit times obtained from this patient’s full-field ERG recordings performed in 1995 when he was tested in October 2005.

Optical coherence tomography of the retina showed that the patient had well-preserved outer segments (OS) and photoreceptor layer, suggesting that there was little or no cell death (data reviewed but not shown).

Genotyping

A missense C to A mutation in the first nucleotide of codon 258 was found in the proband (data reviewed but not shown).

Generation of *H258N* Mice

The *H258N* mutant allele of *Pde6b* was hypothesized to act by blocking inhibition of the catalytic core PDE6αβ mediated by the wild-type PDE6γ. To test the effects of *H258N* on PDE6 function in vivo, transgenic lines expressing the *H258N* mutant allele were generated

and backcrossed with FVB (*Pde6b*^{rd1}/*Pde6b*^{rd1}) to obtain mice [*Tg*(*Pde6bH258N*); *Pde6b*^{rd1}/*Pde6b*^{rd1}] that only express the mutant PDE6β. These FVB animals do not have any PDE6β in their rods [Bowes et al., 1990; Pittler and Baehr, 1991]. The standard nomenclature of the *H258N* transgenic mouse should be *Tg*(*Pde6bH258N*); *Pde6b*^{rd1}/*Pde6b*^{rd1}, hereafter referred to as *H258N*. Two independent *H258N* lines were used for this study.

As a control, a line of transgenic mice expressing the wild-type *Pde6b* in the FVB (*Pde6b*^{rd1}/*Pde6b*^{rd1}) genetic background was also examined. This control line manifested similar biochemical and physiological phenotypes as mice carrying *Tg*(*Pde6bH258N*); *Pde6b*$^{rd1/+}$. Initial examinations of *H258N* were conducted in the (B6CBA × FVB) F2 mixed genetic background. Later, to limit any potential variation caused by differences in genetic background, mutant alleles were backcrossed into the DBA strain. N10 from such crosses were used for subsequent physiological assays.

The *H258N* allele generated 260- and 80-bp fragments following restriction HincII digestion of the nested PCR product, while the *Pde6b*^{rd1} allele produced a 340-bp product in this reaction. *H258N* mice demonstrate a heterozygous pattern after digestion with HincII.

Biochemical Analyses of Mutant Mice

Immunoblots of rod outer segments (ROS) of each transgenic line, normalized by the amount of rhodopsin present, revealed that levels of *H258N* mutant PDE6β were similar in both lines to PDE6β levels of control C57BL/6 (+/+) mice (Fig. 2). In addition, levels of PDE6αβ were similar to those in C57BL/6 control (+/+) ROS (Fig. 2). Therefore, both of the *H258N* founder lines were used in subsequent experiments.

H258N mice showed an increased rate of retinal cGMP hydrolysis in the dark (basal activity). The activity of cGMP-PDE6 was 319.2 nmol × min^{-1} × nmol^{-1} rhodopsin in mutant animals compared to 130.1 nmol × min^{-1} × nmol^{-1} rhodopsin in wild-type controls. This result demonstrates that the *H258N* mutation alters the ability of PDE6γ to bind and inhibit the PDE6αβ catalytic core, consistent with previously published data [Muradov et al., 2003].

Phenotypic Analyses of *H258N* Mice

Slit lamp examinations of anterior and posterior segments of *H258N* mice were clinically indistinguishable from wild type. An abnormal eye axial length is one of the earliest clinical manifestations of human CSNB; it is detected as a myopic refractive error in neonates, in contrast with a typical infant's hyperopic refractive error. While emmetropization occurs in most normal individuals by early childhood, a myopic refractive error persists in CSNB patients. To determine whether *H258N* mice displayed similar features, streak retinoscopy was performed as previously described (Tejedor and de la Villa, 2003]. The spherical equivalent retinoscopic refraction in control mice was 13.89 ± 0.85 diopters (mean ± standard deviation); in *H258N* mice, it was 17.71±0.86 diopters. The hyperopic difference corresponded appropriately to a decreased eye axial length (data not shown) [Tejedor and de la Villa, 2003]. Thus, the mouse model exhibits a refractive error distinct from that seen in human CSNB.

Degeneration *Pde6b*^{rd1}/*Pde6b*^{rd1} Mice

Histological sections prepared from 6-month-old mouse retina showed from 10 to 12 rows of photoreceptor nuclei in both *Tg*(*Pde6bH258N*); *Pde6b*$^{rd1/+}$ and *H258N* in either (B6CBA × FVB) F2 or DBA backgrounds. On the other hand, parental homozygous *Pde6b*^{rd1}/*Pde6b*^{rd1} mice without the *H258N* transgene showed complete photoreceptor degeneration at 3 months of age (Fig. 3). Thus, degeneration of *Pde6b*^{rd1}/*Pde6b*^{rd1} photoreceptors was rescued by the mutant *H258N* transgene as determined by light (Fig. 3) and electron microscopy (Fig. 4). As

expected, the wild-type *Pde6b* control transgene also rescued $Pde6b^{rd1}/Pde6b^{rd1}$ photoreceptors (data not shown).

Panretinal Physiological Features of *H258N* Mice on (B6CBA × FVB) F2 Hybrid Background

To assess retinal function in *H258N* mice on the (B6CBA × FVB) F2 hybrid background, ERGs were recorded from *H258N* and heterozygous $Pde6b^{rd1}/+$ control mice (rd1/+). ERGs obtained from *Tg*(*Pde6bH258N*); $Pde6b^{rd1/+}$ mice are within normal limits (data not shown). A fit of a rod model to the *a*-wave of the ERG did not reveal a significant difference between the mutants and controls in Rm_{p3}, the saturated *a*-wave amplitude, and log *S*, the sensitivity of the rod-mediated photoresponse; there was, however, a trend in the direction of reduced amplitudes and sensitivity for the *H258N* mice (Table 1, Fig. 5). In contrast, *H258N* mice demonstrated more severe losses at the level of the *b*-wave of the ERG. V_{max}, the saturated *b*-wave amplitude obtained from a Naka-Rushton fit, is in *H258N* mutant mice approximately half that of $Pde6^{rd1}/+$ heterozygous controls (Table 1, *k*Fig. 5C), and retinal sensitivity, , is shifted by 0.23 log units. As an index of the selective loss of the *b*-wave on the ERG, we calculated the ratio Rm_{P3}/V_{max}. For wild-type and $Pde6^{rd1}/+$ heterozygous controls this ratio was 1.15 and 1.13, respectively; for mutant mice, the ratio was 0.73. Finally, serial ERG testing shows a slight progression over time in all parameters; however, these changes parallel those observed in wild-type and heterozygous controls—consistent with stationary disease and normal aging of the retina (Fig. 5B).

Panretinal Physiological Features of *H258N* Mice on DBA Background

To assess physiological responses of *H258N* mice on a DBA background (Fig. 6), ERGs were recorded from *H258N* and normal DBA control mice (+/+) (Fig. 6). ERGs recorded from *H258N* mutants were abnormal for all mice tested. On average, V_{max} was 82.2 and 285 mV for *H258N* and control mice, respectively. Despite the overall abnormal ERG responses, there was no evidence in any mice of selective loss at the level of the *b*-wave of the ERG. On average, the *b*- to *a*-wave amplitude ratio for the most intense stimulus was 2.4 ± 0.7.

Single-Cell Recording of *H258N* Mice on (B6CBA × FVB) F2 Hybrid Background

The responses of single rods from mice carrying the *H258N* mutation were also normal, exhibiting similar amplitudes and waveforms (Fig. 7, Tables 2 and 3). There were no significant differences in latency, time-to-peak, or saturating current amplitude (Student's t-test; $P = 0.05$). When peak amplitudes to a number of light intensities were normalized to the maximum (saturating) current amplitude, averaged, and plotted together (Fig. 7B), there was a small difference in the position of the curve for control and mutant rods along the axis for light intensity, indicating that *H258N* rods were slightly less sensitive. This difference is unlikely to be significant; however, since when we calculated the single-photon response from a different sample of control and *H258N* rods, the mutant response was somewhat larger (Fig. 7C, Table 2). The normalised single-photon responses of control and mutant rods were identical in waveform (Fig. 7C). Thus, *H258N* rods have normal function in the (B6CBA × FVB) F2 hybrid background.

DISCUSSION

In 1994, members of a large Danish kindred with CSNB were reported to have a C-to-A transversion in exon 4 of the *PDE6B* gene (Gal et al., 1994]. This nucleotide substitution in codon 258 is located in a conserved region between two GAP domains adjacent to the reported PDE6γ-interacting domain. In frogs, interaction between the GAF domains on PDE6αβ and PDE6γ regulates the duration of PDE6 activity [Arshavsky et al., 1992]. PDE6γ-dependent inhibition of PDE6 is compromised in *H258N* rods and should result in a higher basal level of PDE activity [Muradov et al., 2003], thereby accounting for the CSNB phenotype found in the

Danish kindred. Another allele within the GAP domain, L228H, results in a change from a neutral hydrophobic leucine to a basic hydrophilic residue [Danciger et al., 1995; Gao et al., 1996], and is associated with RP.

Pde6b^{rd1}/*Pde6b*^{rd1} mice carry a homozygous nonsense mutation in codon 347 [Pittler and Baehr, 1991], in addition to a transcriptionally active murine leukemia virus (MuLV)-Xmv28 [Bowes et al., 1990] in intron 1 of *Pde6b.* While *Pde6b*^{rd1}/*Pde6b*^{rd1} mice have severe photoreceptor degeneration resembling RP, transgenic *H258N* mice display normal photoreceptor morphology (Fig. 4). Although the *H258N* mutant transgene rescued cell death caused by *Pde6b*^{rd1}, the cGMP-PDE6 of dark-adapted *H258N* OSs showed an abnormal three-fold increase in the rate of retinal cGMP hydrolysis compared to controls. The elevated PDE6 activity in *H258N* could increase photoreceptor noise in darkness. Rieke and Baylor [2000] have estimated that half of the dark noise in rods derives from spontaneously activated rhodopsin, and that most of the remaining noise results from activated PDE6. Thermal activation of rhodopsin contributes to the discrete noise, while spontaneous PDE6 activation accounts for the continuous noise [Lamb, 1987]. A single PDE6 molecule becomes spontaneously activated about once every hour; the rate constant for spontaneous PDE6 activation is $k_1 = 4 \times 10^{-4}\ s^{-1}$. The frequency of PDE6 activation is critical for reproducible single photon detection. Increased spontaneous dark PDE6 activity accounts for the increased dark noise and lack of saturation under steady illumination [Barlow, 1972] in cones as opposed to rods [Holcman and Korenbrot, 2005]. Similarly, increased spontaneous dark PDE6 activity in *H258N* could light-adapt photoreceptors in a CSNB patient.

Our CSNB patient's ERG examination was consistent with generalized retinal dysfunction affecting the rod system and the rod-bipolar interphase—possibly due to increased dark PDE6 noise. Increasing stimulus intensity leads to partial restoration of the maximal *b*-wave, suggesting that not all photoreceptor-bipolar cell connections are disrupted in our *H258N* proband. Optical coherence tomography imaging of the retina showed no cell loss in this 36-year-old patient. In the albino (B6CBA × FVB) F2 hybrid background, ERGs from the *H258N* mice were similar to those obtained from our CSNB patient. They were also similar to humans with the most common form of CSNB (X-linked), that usually demonstrate a marked selective loss of the *b*-wave with relatively normal *a*-waves (i.e., an electronegative type of ERG); the defect in X-linked CSNB has been suggested to lie downstream to the photoreceptor neurons, possibly in the ON-bipolar cells or their interconnections [Hood and Birch, 1996]. The sensitivity of ON-bipolar cells may be limited by their increased PDE6 dark activity and the consequent photoreceptor noise, thereby diminishing the optimal interpretation of signal-to-noise and, ultimately, visual sensitivity—as seen in some Rambusch family members [Rosenberg et al., 1991].

Unexpectedly, DBA inbred mice carrying the *H258N* mutant allele did not demonstrate a selective loss of *b*-wave from ON-bipolar cells. Instead, uniform amplitude reductions in both *a*- and *b*-wave components resulted from increased dark cGMP PDE6 activity due to impaired inactivation of *H258N* by PDE6γ. Therefore, the *H258N* allele can have markedly different phenotypes when placed on different backgrounds.

Olfaction, for example, utilizes a similar G protein-coupled receptor signaling system and also displayed variation on different genetic backgrounds [Lee et al., 2003]. Likewise, different genetic backgrounds modulate the function of keratin 8 (K8). In the C57Bl/6x129Sv mixed background, the null K8 mutation causes midgestational lethality [Baribault et al., 1994]. In the FVB/N strain background, however, K8 null mice develop to adulthood [Baribault et al., 1994]. Genetic background also varies the incidence of thymoma associated with the p53 null allele [van Meyel et al., 1998], and the number of polyps caused by the multiple intestinal neoplasia allele of the murine adenomatous polyposis coli gene. One modifier locus. *Mom1*,

confers tumor resistance by encoding a locally active secretory phospholipase [Haines et al., 2005; Halberg et al., 2000; MacPhee et al., 1995; Shoemaker et al., 1998]. A second modifier locus, *Dnmt*, seems to control, by DNA methylation, the activity of a negative regulator of tumor growth [Eads et al., 2002]. Allelic variants in the FVB, CBA, C57BL6, or DBA genomes have significant impact on ERG and physiological manifestations of *H258N*. These variants, encoded by modifier genes in various genetic backgrounds, are the basis of genetic diversity [Banbury Conference, 1997; Bothe et al., 2004; Clapcote and Roder, 2004; Erickson, 1996; Le Roy et al., 2000; Linder, 2001; Rodgers et al., 2002; Schauwecker, 2002; Sigmund, 2000]. To avoid the confounding issue of variation resulting from differences in genetic background, there is a movement to create all transgenic mice in the same inbred background [Austin et al., 2004].

The considerable phenotypic variability in residual rod activity in the dark in affected members of the Rambusch family may also be attributable to differences in genetic background. The deviation of bright flash ERGs in the six index CSNB patients in the Rambusch family reflected different degrees of disease expression, and varying degrees of electronegativity [Rosenberg et al., 1991]. Thus, the fact that expression of CSNB is heterogeneous in Rambusch family members [Rosenberg et al., 1991] with the same *H258N* mutation, indicates that factors other than the *PDE6B* gene itself contribute to the pathophysiology of this retinal dystrophy.

Acknowledgments

We thank Frank D. Costantini, Gordon L. Fain, Vivienne C. Greenstein, Meisheng Jiang, and members of their laboratories for sharing ideas and equipment, as well as for critical reading of the manuscript. We also thank Peter Gouras for guidance and advice and members of the Farber and Fain laboratories for support—especially Won-Ho Lee and Hong Mei Dong. S.H.T. is a Fellow of the Burroughs-Wellcome Program in Biomedical Sciences, and is supported by the Foundation Fighting Blindness, the Eye Surgery Fund, the Jahnigen Award from the American Geriatrics Society, the Hirschl Charitable Trust, the Becker/Association of University Professors in Ophthalmology/Research to Prevent Blindness (RPB), and NIH-EY004081. M.L. is supported by a Patient-Oriented Diabetes Research Career Award from the Juvenile Diabetes Research Foundation (Grant number 8-2002-130). S.PG. is an investigator of the Howard Hughes Medical Institute.

Grant sponsor: Foundation Fighting Blindness; Grant sponsor: Eye Surgery Fund; Grant sponsor: American Geriatrics Society (Jahnigen Award); Grant sponsor: Hirschl Charitable Trust; Becker/Association of University Professors in Ophthalmology/Research to Prevent Blindness (RPB); Grant sponsor: National Institutes of Health (NIH); Grant number: EY004081; Grant sponsor: Juvenile Diabetes Research Foundation (Patient-Oriented Diabetes Research Career Award); Grant number: 8-2002-130.

References

Arshavsky VY, Dumke CL, Bownds MD. Noncatalytic cGMP-binding sites of amphibian rod cGMP phosphodiesterase control interaction with its inhibitory γ-subunits. A putative regulatory mechanism of the rod photoresponse. J Biol Chem 1992;267:24501–24507. [PubMed: 1332960]

Arshavsky VY, Lamb TD, Pugh EN Jr. G proteins and photo-transduction. Annu Rev Physiol 2002;64:153–187. [PubMed: 11826267]

Austin CP, Battey JF, Bradley A, Bucan M, Capecchi M, Collins FS, Dove WF, Duyk G, Dymecki S, Eppig JT, Grieder FB, Heintz N, Hicks G, Insel TR, Joyner A, Koller BH, Lloyd KC, Magnuson T, Moore MW, Nagy A, Pollock JD, Roses AD, Sands AT, Seed B, Skarnes WC, Snoddy J, Soriano P, Stewart DJ, Stewart F, Stillman B, Varmus H, Varticovski L, Verma IM, Vogt TF, von Melchner H, Witkowski J, Woychik RP, Wurst W, Yancopoulos GD, Young SG, Zambrowicz B. The knockout mouse project. Nat Genet 2004;36:921–924. [PubMed: 15340423]

Baehr W, Devlin MJ, Applebury ML. Isolation of bovine ROS phosphodiesterase. J Biol Chem 1979;254:11669–11677. [PubMed: 227876]

Bailey, DW. Phylogenetic analysis. In: Morse, HC., editor. Origins of inbred mice. New York: Academic Press: Wiley-Interscience; 1978. p. 15

Banbury Conference. Mutant mice and neuroscience: recommendations concerning genetic background. Banbury Conference on Genetic Background in Mice. Neuron 1997;19:755–759. [PubMed: 9354323]

Baribault H, Penner J, lozzo RV, Wilson-Heiner M. Colorectal hyperplasia and inflammation in keratin 8-deficient FVB/N mice. Genes Dev 1994;8:2964–2973. [PubMed: 7528156]

Barlow, HB. Dark and light adaptation: psychophysics. In: Jameson, D.; Hurvich, LM., editors. Handbook of sensory physiology. Berlin: Springer; 1972. p. 1-28.

Bayer AU, Neuhardt T, May AC, Martus P, Maag KP, Brodie S, Lutjen-Drecoll E, Podos SM, Mirtag T. Retinal morphology and ERG response in the DBA/2NNia mouse model of angle-closure glaucoma. Invest Ophthalmol Vis Sci 2001;42:1258–1265. [PubMed: 11328737]

Baylor DA, Lamb TD, Yau KW. Responses of retinal rods to single photons. J Physiol (Lond) 1979;288:613–634. [PubMed: 112243]

Bitensky MW, Miki N, Keirns JJ, Keirns M, Baraban JM, Freeman J, Wheeler MA, Lacy J, Marcus FR. Activation of photoreceptor disk membrane phosphodiesterase by light and ATP. Adv Cyclic Nucleotide Res 1975;5:213–240. [PubMed: 165667]

Bothe GW, Bolivar VJ, Vedder MJ, Geistfeld JG. Genetic and behavioral differences among five inbred mouse strains commonly used in the production of transgenic and knockout mice. Genes Brain Behav 2004;3:149–157. [PubMed: 15140010]

Bowes C, Li T, Danciger M, Baxter LC, Applebury ML, Farber DB. Retinal degeneration in the rd mouse is caused by a defect in the β subunit of rod cGMP phosphodiesterase. Nature 1990;347:677–680. [PubMed: 1977087]

Burns ME, Baylor DA. Activation, deactivation, and adaptation in vertebrate photoreceptor cells. Annu Rev Neurosci 2001;24:779–805. [PubMed: 11520918]

Burns ME, Arshavsky VY. Beyond counting photons: trials and trends in vertebrate visual transduction. Neuron 2005;48:387–401. [PubMed: 16269358]

Chen J, Flannery JG, La Vail MM, Steinberg RH, Xu J, Simon MI. BCL-2 overexpression reduces apoptotic photoreceptor cell death in three different retinal degenerations. Proc Natl Acad Sci USA 1996;93:7042–7047. [PubMed: 8692941]

Clapcote SJ, Roder JC. Survey of embryonic stem cell line source strains in the water maze reveals superior reversal learning of 129S6/SvEvTac mice. Behav Brain Res 2004;152:35–48. [PubMed: 15135967]

Cote RH. Kinetics and regulation of cGMP binding to noncatalytic binding sites on photoreceptor phosphodiesterase. Methods Enzymol 2000;315:646–672. [PubMed: 10736732]

D'Amours MR, Cote RH. Regulation of photoreceptor phosphodiesterase catalysis by its non-catalytic cGMP-binding sites. Biochem J 1999;340(Pt 3):863–869. [PubMed: 10359674]

Danciger M, Blaney J, Gao Y, Zhao D, Heckenlively J, Jacobson S, Farber D. Mutations in the PDE6B gene in autosomal recessive retinitis pigmentosa. Genomics 1995;30:1–7. [PubMed: 8595886]

Dryja TR, Hahn LB, Reboul T, Arnaud B. Missense mutation in the gene encoding the alpha subunit of rod transducin in the Nougaret form of congenital stationary- night blindness. Nat Genet 1996;13:358–360. [PubMed: 8673138]

Eads CA, Nickel AE, Laird PW. Complete genetic suppression of polyp formation and reduction of CpG-island hypermethylation in Apc (Min/+) Dnmt1-hypomorphic mice. Cancer Res 2002;62:1296–1299. [PubMed: 11888894]

Erickson RR. Mouse models of human genetic disease: which mouse is more like a man? Bioessays 1996;18:993–998. [PubMed: 8976156]

Fain GL, Matthews HR, Cornwall MC, Koutalos Y. Adaptation in vertebrate photoreceptors. Physiol Rev 2001;81:117–151. [PubMed: 11152756]

Farber DB, Lolley RN. Enzyme basis for cyclic GMP accumulation in degenerative photoreceptor cells of mouse retina. J Cyclic Nucleotide Res 1976;2:139–148. [PubMed: 6493]

Fung BKK, Hurley JB, Stryer L. Flow of information in the light-triggered cyclic nucleotide cascade of vision. Pro Natl Acad Sci USA 1981;78:152–156.

Fung BKK, Young JH, Yamane HK, Griswold-Prenner I. Subunit stoichiometry of retinal rod cGMP phosphodiesterase. Biochemistry 1990;29:2657–2664. [PubMed: 2161252]

Gal A, Orth U, Baehr W, Schwinger E, Rosenberg T. Heterozygous missense mutation in the rod cGMP phosphodiesterase β-subunit in autosomal dominant stationary night blindness. Nat Genet 1994;7:64–68. [PubMed: 8075643]

Gao YQ, Danciger M, Zhao DY, Blaney J, Piriev NI, Shih J, Jacobson SG, Heckenlively JH, Farber DB. Screening of the PDE6B gene in patients with autosomal dominant retinitis pigmentosa. Exp Eye Res 1996;62:149–154. [PubMed: 8698075]

Guo LW, Grant JE, Hajipour AR, Muradov H, Arbabian M, Artemyev NO, Ruoho AE. Asymmetric interaction between rod cyclic GMP phosphodiesterase gamma subunits and alpha/beta subunits. J Biol Chem 2005;280:12585–12592. [PubMed: 15668239]

Guo LW, Muradov H, Hajipour AR, Sievert MK, Artemyev NO, Ruoho AE. The inhibitory gamma subunit of the rod cGMP phosphodiesterase binds the catalytic subunits in an extended linear structure. J Biol Chem 2006;281:15412–15422. [PubMed: 16595671]

Haines J, Johnson V, Pack K, Suraweera N, Slijepcevic P, Cabuy E, Coster M, Ilyas M, Wilding J, Sieber O, Bodmer W, Tomlinson I, Silver A. Genetic basis of variation in adenoma multiplicity in ApcMin/+Mom1S mice. Proc Natl Acad Sci USA 2005;102:2868–2873. [PubMed: 15710876]

Halberg RB, Katzung DS, Hoff PD, Moser AR, Cole CE, Lubet RA, Donehower LA, Jacoby RF, Dove WE. Tumorigenesis in the multiple intestinal neoplasia mouse: redundancy of negative regulators and specificity of modifiers. Proc Natl Acad Sci USA 2000;97:3461–3466. [PubMed: 10716720]

Holcman D, Korenbrot JI. The limit of photoreceptor sensitivity: molecular mechanisms of dark noise in retinal cones. J Gen Physiol 2005;125:641–660. [PubMed: 15928405]

Hood DC, Birch DG. Beta wave of the scotopic (rod) electroretinogram as a measure of the activity of human on-bipolar cells. J Opt Soc Am A 1996;13:623–633.

Kamps KM, Hofmann KP. ATP can promote activation and deactivation of the rod cGMP-phosphodiesterase. Kinetic light scattering on intact rod outer segments. FEBS Lett 1986;208:241–247. [PubMed: 3023137]

Lamb TD. Sources of noise in photoreceptor transduction. J Opt Soc Am A 1987;4:2295–2300. [PubMed: 3430216]

Le Roy I, Pothion S, Mortaud S, Chabert C, Nicolas L, Cherfouh A, Roubertoux PL. Loss of aggression, after transfer onto a C57BL/6J background, in mice carrying a targeted disruption of the neuronal nitric oxide synthase gene. Behav Genet 2000;30:367–373. [PubMed: 11235982]

Lee AW, Emsley JG, Brown RE, Hagg T. Marked differences in olfactory sensitivity and apparent speed of forebrain neuroblast migration in three inbred strains of mice. Neuroscience 2003;118:263–270. [PubMed: 12676156]

Lem J, Applebury ML, Falk JD, Flannery JG, Simon Ml. Tissue-specific and developmental regulation of rod opsin chimeric genes in transgenic mice. Neuron 1991;6:201–210. [PubMed: 1825171]

Lem J, Fain GL. Constitutive opsin signaling: night blindness or retinal degeneration? Trends Mol Med 2004;10:150–157. [PubMed: 15059605]

Linder CC. The influence of genetic background on spontaneous and genetically engineered mouse models of complex diseases. Lab Anim (NY) 2001;30:34–39. [PubMed: 11385732]

MacPhee M, Chepenik KP, Liddell RA, Nelson KK, Siracusa LD, Buchberg AM. The secretory phospholipase A2 gene is a candidate for the Moml locus, a major modifier of ApcMin-induced intestinal neoplasia. Cell 1995;81:957–966. [PubMed: 7781071]

Marmor, M.; Holder, G.; Seeliger, M.; Yamamoto, S. Standard for clinical electroretinography; Doc Opthalmol. 2004. p. 117-114.[2004 update]Available at: http://www.iscev.org/standards

McLaughlin ME, Sandberg MA, Berson EL, Dryja TP. Recessive mutations in the gene encoding the β-subunit of rod phosphodiesterase in patients with retinitis pigmentosa. Nat Genet 1993;4:130–134. [PubMed: 8394174]

McLaughlin ME, Ehrhart TL, Berson EL, Dryja TP. Mutation spectrum of the gene encoding the β-subunit of rod phosphodiesterase among patients with autosomal recessive retinitis pigmentosa. Proc Nat Acad Sci USA 1995;92:3249–3253. [PubMed: 7724547]

Mou H, Grazio HJ 3rd, Cook TA, Beavo JA, Cote RH. cGMP binding to noncatalytic sites on mammalian rod photoreceptor phosphodiesterase is regulated by binding of its gamma and delta subunits. J Biol Chem 1999;274:18813–18820. [PubMed: 10373499]

Mou H, Cote RH. The catalytic and GAF domains of the rod cGMP phosphodiesterase (PDE6) heterodimer are regulated by distinct regions of its inhibitory gamma subunit. J Biol Chem 2001;276:27527–27534. [PubMed: 11375400]

Moussaif M, Rubin WW, Kerov V, Reh R, Chen D, Lem J, Chen CK, Hurley JB, Burns ME, Artemyev NO. Phototransduction in a transgenic mouse model of Nougaret night blindness. J Neurosci 2006;26:6863–6872. [PubMed: 16793893]

Muradov KG, Granovsky AE, Artemyev NO. Mutation in rod PDE6 linked to congenital stationary night blindness impairs the enzyme inhibition by its gamma-subunit. Biochemistry 2003;42:3305–3310. [PubMed: 12641462]

Norton AW, D'Amours MR, Grazio HJ, Hebert TL, Cote RH. Mechanism of transducin activation of frog rod photoreceptor phosphodiesterase. Allosteric interactions between the inhibitory gamma subunit and the noncatalytic cGMP-binding sites. J Biol Chem 2000;275:38611–38619. [PubMed: 10993884]

Peterson GL. A simplification of the protein assay method of Lowry et al. which is more generally applicable. Anal Biochem 1977;83:346–356. [PubMed: 603028]

Piccolino FC, Calabria G, Polizzi A, Fioretto M. Pigmentary retinal dystrophy associated with pigmentary glaucoma. Graefes Arch Clin Exp Ophthalmol 1989;227:335–339. [PubMed: 2476365]

Piriev NI, Yamashita C, Samuel G, Farber DB. Rod photoreceptor cGMP-phosphodiesterase: Analysis of α and β subunits expressed in human kidney cells. Pro Natl Acad Sci USA 1993;90:9340–9344.

Pittler SJ, Baehr W. Identification of a nonsense mutation in the rod photoreceptor cGMP phosphodiesterase β-subunit gene of the rd mouse. Proc Nat Acad Sci USA 1991;88:8322–8326. [PubMed: 1656438]

Rieke, F.; Baylor, DA. Neuron. Vol. 26. 2000. Origin and functional impact of dark noise in retinal cones; p. 181-186.

Rodgers RJ, Boullier E, Chatzimichalaki P, Cooper GD, Shorten A. Contrasting phenotypes of C57BL/6JOlaHsd, 129S2/SvHsd and 129/SvEv mice in two exploration-based tests of anxiety-related behaviour. Physiol Behav 2002;77:301–310. [PubMed: 12419406]

Rosenberg T, Haim M, Piczenik Y, Simonsen SE. Autosomal dominant stationary night-blindness. A large family rediscovered. Acta Ophthalmol (Copenh) 1991;69:694–702. [PubMed: 1789082]

Sandberg MA, Pawlyk BS, Dan J, Arnaud B, Dryja TP, Berson EL. Rod and cone function in the Nougaret form of stationary night blindness. Arch Ophthalmol 1998;116:867–872. [PubMed: 9682699]

Schauwecker PE. Complications associated with genetic background effects in models of experimental epilepsy. Prog Brain Res 2002;135:139–148. [PubMed: 12143336]

Schuettauf F, Rejdak R, Walski M, Frontczak-Baniewicz M, Voelker M, Blatsios G, Shinoda K, Zagorski Z, Zrenner E, Grieb P. Retinal neurodegeneration in the DBA/2J mouse-a model for ocular hypertension. Acta Neuropathol (Berl) 2004;107:352–358. [PubMed: 14745571]

Shoemaker AR, Moser AR, Midgley CA, Clipson L, Newton MA, Dove WF. A resistant genetic background leading to incomplete penetrance of intestinal neoplasia and reduced loss of heterozygosity in ApcMin/+mice. Proc Natl Acad Sci USA 1998;95:10826–10831. [PubMed: 9724789]

Sigmund CD. Viewpoint: are studies in genetically altered mice out of control? Arterioscler Thromb Vasc Biol 2000;20:1425–1429. [PubMed: 10845854]

Slep KC, Kercher MA, He W, Cowan CW, Wensel TG, Sigler PB. Structural determinants for regulation of phosphodiesterase by a G protein at 2.0 A. Nature 2001;409:1071–1077. [PubMed: 11234020]

Sorscher EJ, Huang Z. Diagnosis of genetic disease by primer-specified restriction map modification, with application to cystic fibrosis and retinitis pigmentosa. Lancet 1991;337:1115–1118. [PubMed: 1674012]

Stryer L. Visual excitation and recovery. J Biol Chem 1991;266:10711–10714. [PubMed: 1710212]

Tejedor J, de la Villa P. Refractive changes induced by form deprivation in the mouse eye. Invest Ophthalmol Vis Sci 2003;44:32–36. [PubMed: 12506052]

Towbin H, Staehelin T, Gordon J. Electrophoretic transfer of proteins from polyacrylamide gels to nitrocellulose sheets: procedure and some applications. Proc Natl Acad Sci USA 1979;76:4350–4354. [PubMed: 388439]

Tsang SH, Gouras P, Yamashita CK, Kjeldbye H, Fisher J, Farber DB, Goff SP. Retinal degeneration in mice lacking the γ subunit of rod cGMP phosphodiesterase. Science 1996;272:1026–1029. [PubMed: 8638127]

Tsang, SH.; Burns, ME.; Calvert, PD.; Gouras, P.; Baylor, DA.; Goff, SP.; Arshavsky, VY. Science. Vol. 282. 1998. Role of the target enzyme in deactivation of photoreceptor G protein in vivo; p. 117-121.

Tsang, SH.; Gouras, P. Photoreceptors and photoreceptor dysfunctions. In: Adelman, G.; Smith, B., editors. Encyclopedia of neuroscicnce. Amsterdam: Elsevier Science; 1999. p. 1633-1644.

Tsang SH, Woodruff ML, Chen CK, Yamashita CY, Cilluffo MC, Rao AL, Farber DB, Fain GL. GAP-independent termination of photoreceptor light response by excess gamma subunit of the cGMP-phosphodiesterase. J Neurosci 2006;26:4472–4480. [PubMed: 16641226]

van Meyel DJ, Sanchez-Sweatman OH, Kerkvliet N, Stitt L, Ramsay DA, Khokha R, Chambers AF, Cairncross JG. Genetic background influences timing, morphology and dissemination of lymphomas in p53-deficient mice. Int J Oncol 1998;13:917–922. [PubMed: 9772279]

Wakayama S, Kishigami S, Van Thuan N, Ohta H, Hikichi T, Mizutani E, Yanagimachi R, Wakayama T. Propagation of an infertile hermaphrodite mouse lacking germ cells by using nuclear transfer and embryonic stem cell technology. Proc Natl Acad Sci USA 2005;102:29–33. [PubMed: 15618395]

Wensel TG, Stryer L. Reciprocal control of retinal rod cyclic GMP phosphodiesterase by its γ subunit and transducin. Proteins Struct Funct Genet 1986;1:90–99. [PubMed: 2835761]

Woodruff ML, Bownds MD. Amplitude, kinetics, and reversibility of a light-induced decrease in guanosine 3′,5′-cyclic monophosphate in frog photoreceptor membranes. J Gen Physiol 1979;73:629–653. [PubMed: 222877]

Woodruff M, Wang Z, Chung HY, Redmond T, Fain GL, Lem J. Spontaneous activity of opsin apoprotein is a cause of Leber congenital amaurosis. Nat Genet 2003;35:158–164. [PubMed: 14517541]

Yamazaki M, Li N, Bondarenko VA, Yamazaki RK, Baehr W, Yamazaki A. Binding of cGMP to GAF domains in amphibian rod photoreceptor cGMP phosphodiesterase (PDE): identification of GAF domains in frog PDE alpha beta subunits and distinct domains in the PDE gamma subunit involved in the stimulation of cGMP binding to GAF domains. J Biol Chem 2002;11:11.

Yarfitz S, Hurley JB. Transduction mechanisms of vertebrate and invertebrate photoreceptors. J Biol Chem 1994;269:14329–14332. [PubMed: 8182033]

Zhang X, Core RH. cGMP signaling in vertebrate retinal photoreceptor cells. Front Biosci 2005;10:1191–1204. [PubMed: 15769618]

Zimmerman WF, Godchaux WD. Preparation and characterization of sealed bovine rod cell outer segments. Methods Enzymol 1982;81:52–57. [PubMed: 7047993]

Zoraghi R, Corbin JD, Francis SH. Properties and functions of GAF domains in cyclic nucleotide phosphodiesterases and other proteins. Mol Pharmacol 2004;65:267–278. [PubMed: 14742667]

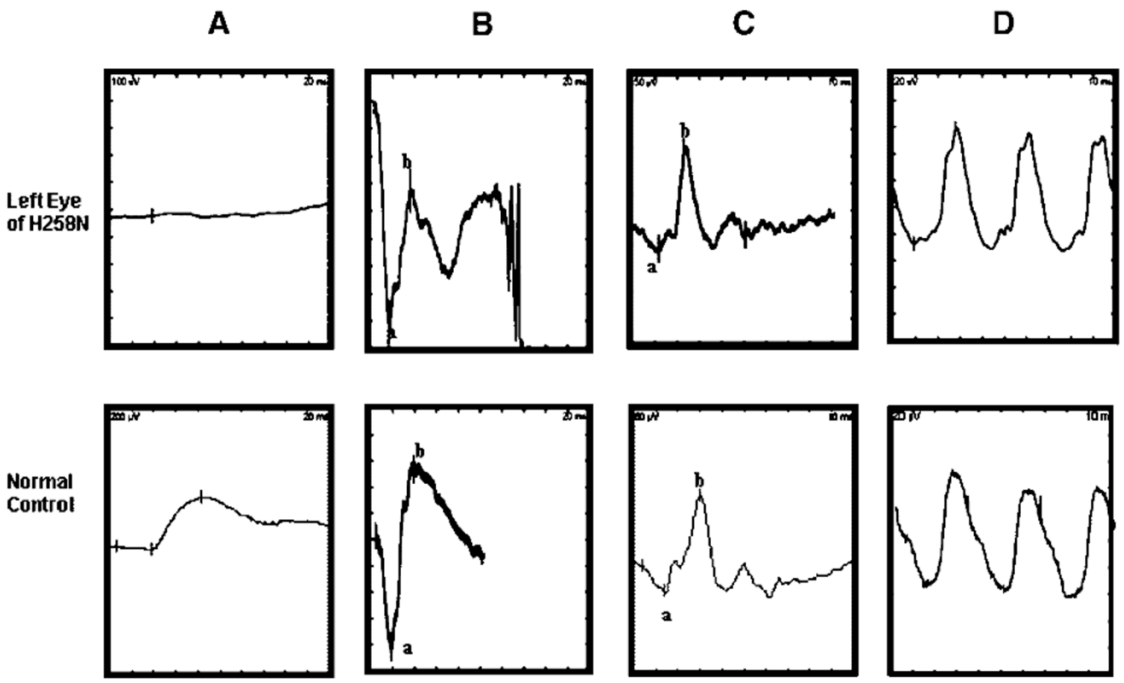

FIGURE 1.

Representative ERG recordings from a patient (top row) and a normal control (bottom row). Shown from left to right are a rod-isolated response (**A**), the dark-adapted maximal response (**B**), the light-adapted responses to a single flash (1 Hz) (**C**) and flickering (30 Hz) stimuli (**D**). *a*- and *b*-waves are identified using conventional techniques. Note the barely detectable rod-isolated response (A) and the selective loss of the *b*-wave for the dark-adapted maximal response in the patient's data (B) compared to the normal control.

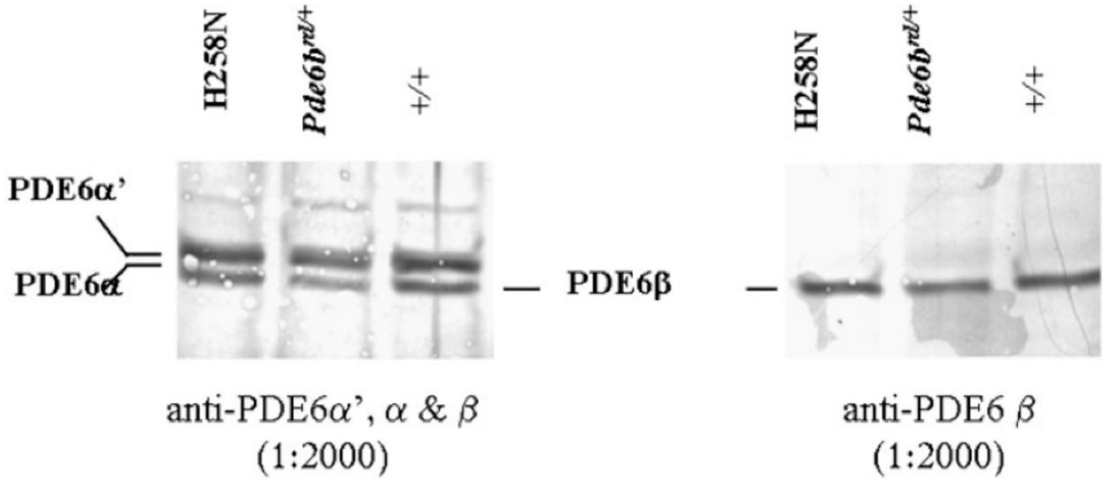

FIGURE 2.

Immunoblot analysis of PDE6 subunit expression in control and *H258N* ROSs. Left panel shows an immunoblot incubated with a polyclonal antibody recognizing both rod PDE6α, PDE6β and cone PDE6α′. Right panel is an immunoblot incubated with a polyclonal antibody specific for rod PDE6β. Protein in all lanes was normalized to 150 pmol rhodopsin. Lane 1, *H258N*; Lane 2, *Pde6b*$^{rd1/+}$; Lane 3, +/+ control.

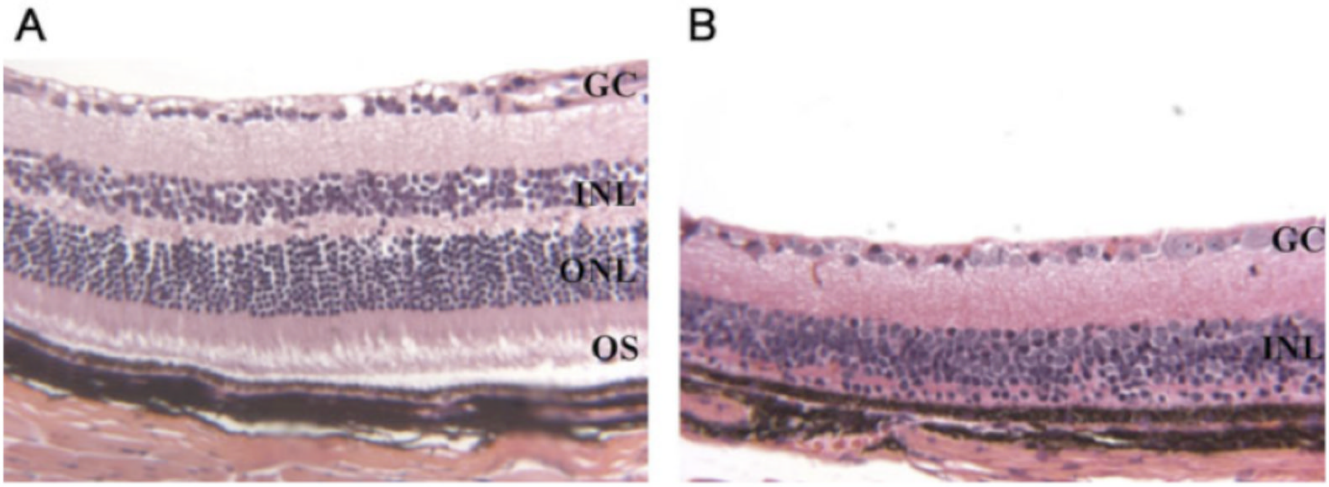

FIGURE 3.

The *H258N* transgene completely rescues photoreceptors in *Pde6b*^{rd1}/*Pde6b*^{rd1} mice. Light micrographs of retina from a 6-month-old *H258N* mouse (**A**) and a 3-month-old homozygote *Pde6b*^{rd1}/*Pde6b*^{rd1} (**B**) in DBA background. OS, outer segments; ONL, outer nuclear layer; INL, inner nuclear layer; GC, ganglion cell layer. OS and ONL comprise the photoreceptor layer. [Color figure can be viewed in the online issue, which is available at www.interscience.wiley.com.)

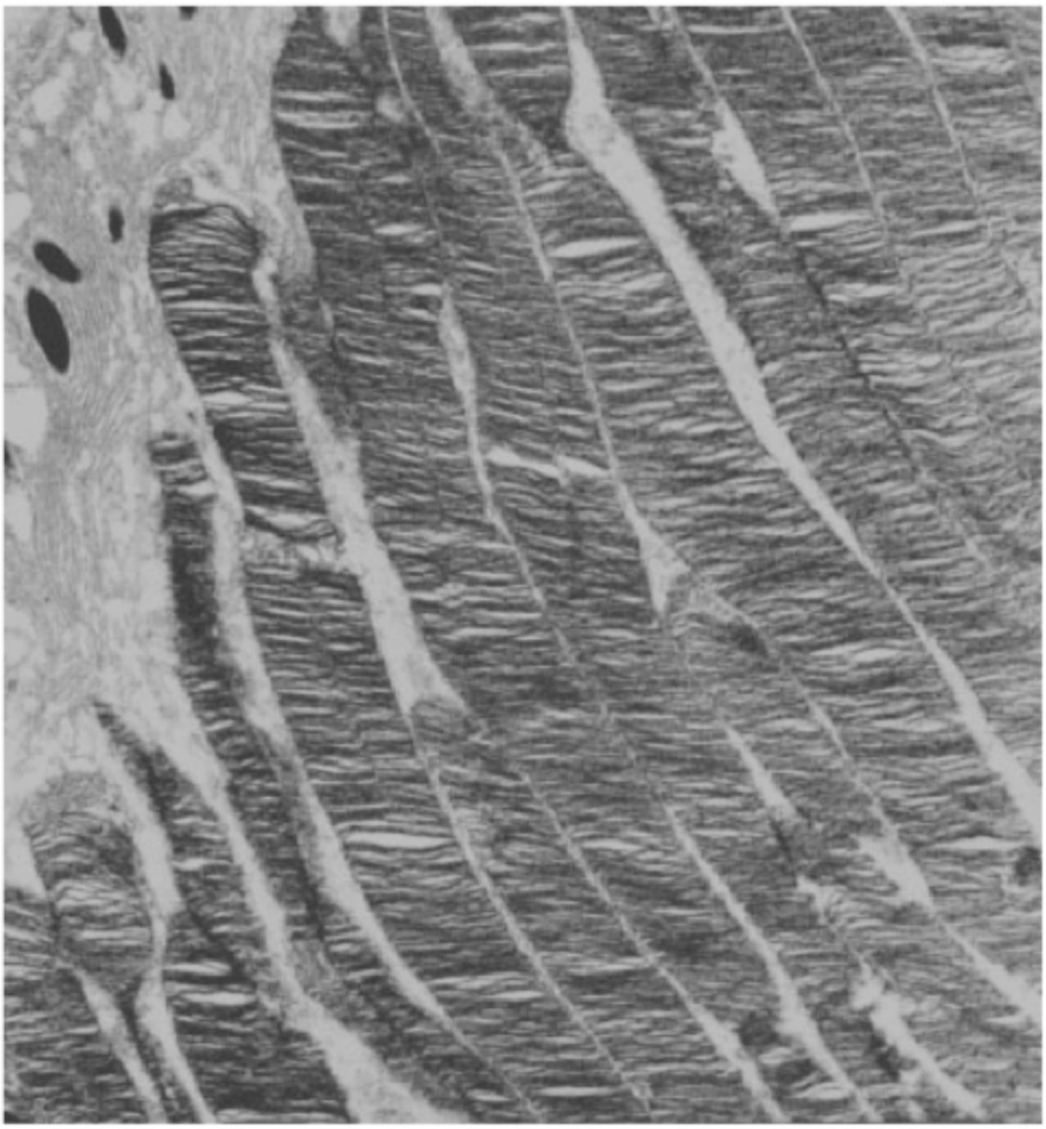

FIGURE 4.
Electron micrograph of retinal section from a 3-month-old *H258N* mouse. The photoreceptor OSs are normal. *Pde6b*^{rd1}/*Pde6b*^{rd1} mice do not have photoreceptors at this age.

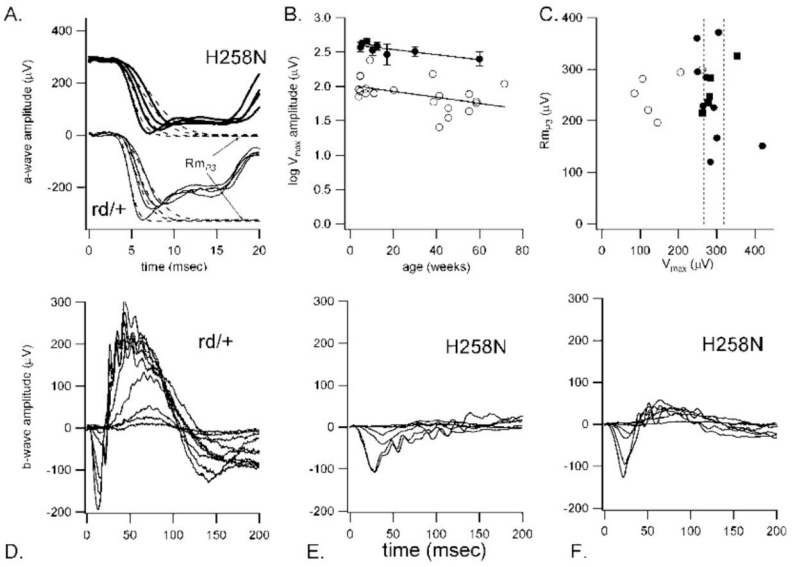

FIGURE 5.

A: Representative panretinal ERG photoresponses from *H258N*, (upper traces) and *Pde6b*^{rd1}/+ control mice (lower traces) on the (B6CBA × FVB) F2 albino background. The dashed lines through each dataset represent the fit of a rod model used to derive Rm_{p3}, the saturated photoreceptor response, and S, photoreceptor sensitivity. **B**: Saturated *b*-wave amplitudes (V_{max}) across age for *H258N* (*open* circles) and wildtype (+/+) control mice (filled circles). **C**: Rm_{p3} vs. V_{max} amplitudes for *H258N* (open circles), *Pde6b*^{rd1}/+ (filled squares) and +/+ control mice (filled circles). The vertical dashed lines are the standard error bars forV_{max} for the +/+ control mice. Note the shift in V_{max} amplitudes to the left, indicating reduced amplitudes for the *H258N* mice. **D–F**: Representative ERGs from *Pde6b*^{rd1}/+ control mice (D), and two *H258N* mutant mice from independent founders in (B6CBA × FVB) F2 albino background(E,F).

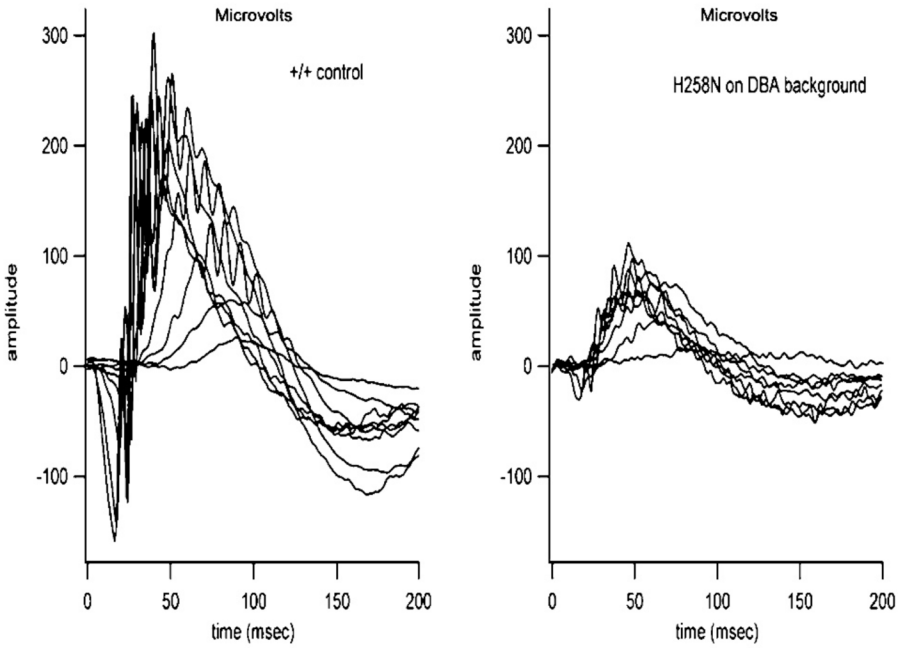

FIGURE 6.

Representative panretinal ERGs from DBA +/+ control mice (left traces) and *H258N* mice (right traces) in the DBA background at 6 months of age.

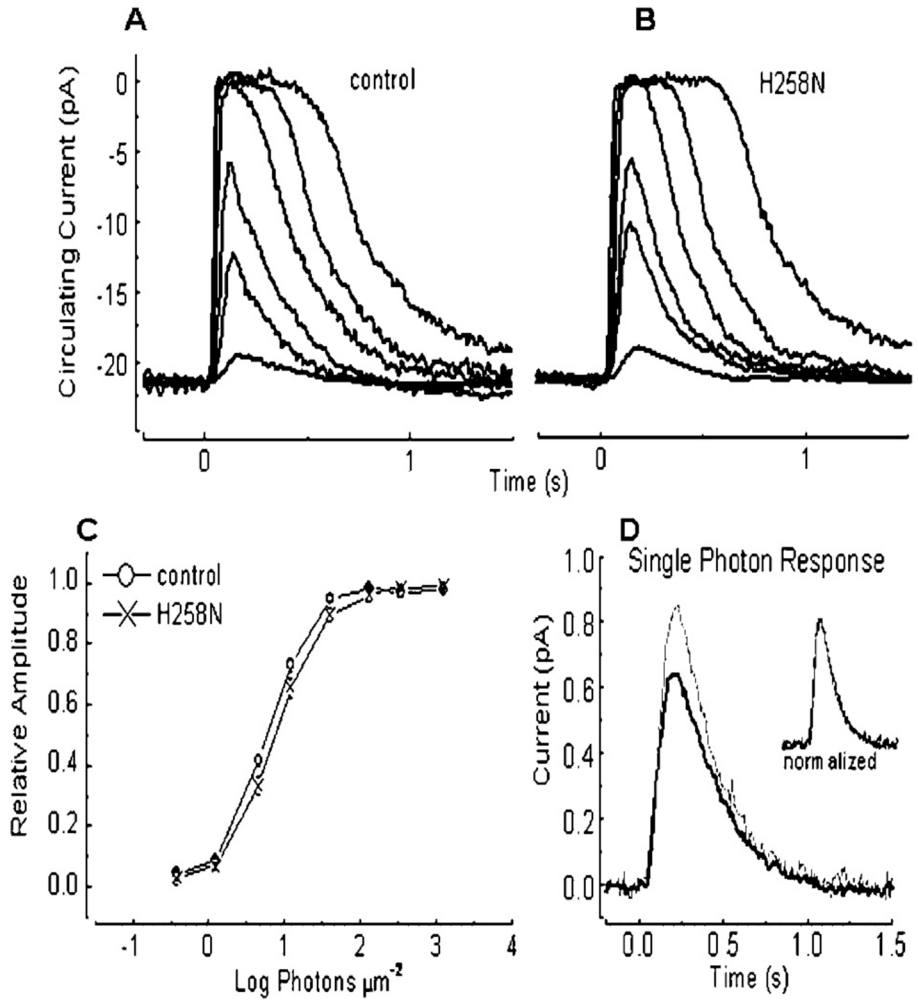

FIGURE 7.

Responses of H258N and control rods to light. **A:** C57BL/6J control rod, 20msec flashes of 500-nm light at flash intensities of 17, 43, 160, 450, 1,120, and 4,230 photons μm^{-2}. The traces are averages of two to four flashes at each intensity. **B:** Typical responses from a H258N rod to the same flash intensities. Each trace was averaged from three to eight flashes. **C:** Response amplitude vs. flash intensity averaged from 34 wild-type (WT; ○) and H258N rods (H258N; X). (The lowest intensity response [smallest response] was obtained by averaging 60 flashes, the others were averaged using five flashes.) **D:** Averaged single-photon responses from H258N (thin line; n = 18) rods superimposed on averaged single-photon response from control rods (thick line; n = 48). Single-photon responses were calculated for each rod individually from 15 to 60 dim flashes with the squared mean-variance method.

TABLE 1

Parameters of ERG Responses in the Human Patient With the *H258N* Allele

	Right eye				Left eye			
	Amplitude (μV)		Implicit times (msec)		Amplitude (μV)		Implicit times (msec)	
ERG	***a*-wave**	***b*-wave**	***a*-wave**	***b*-wave**	***a*-wave**	***b*-wave**	***a*-wave**	***b*-wave**
Dim white (scotopic)	U	U	U	U	U	U	U	U
Blue (scotopic)	U	U	U	U			U	U
Bright white (scotopic)	160.2	84.6	14.0	34.0	126.3	82.0	14.4	34.8
Single flash white (photopic)	33.8	164.1	15.2	29.6	22.1	100.3	15.6	28.8
Flicker 30 Hz (photopic)		106.9		29.0		86.1		28.0

U, undetectable.

Hum Mutat. Author manuscript; available in PMC 2009 September 28.

TABLE 2

Parameters of ERG Responses in the (B6CBA × FVB) F2 Hybrid Background

	V_{max}	log *k*	Rm_{P3}	log S	V_{max}/Rm_{P3}
+/+	292.8 (51.7)	0.0699	245.0 (89.9)	2.3 (0.22)	1.15 (0.37)
Pde6b^{rd1}/+	291.9 (35.6)	0.0592	261.2 (43.9)	2.4 (0.11)	1.13 (0.09)
H258N	154.3 (67.0)	0.1011	213.4 (56.1)	2.1 (0.25)	0.73 (0.24)

TABLE 3

Single-Cell Recording of Rods from H258N Mice in the (B6CBA X FVB) F2 Hybrid Background

	Latency (msec)	Time-to-peak (msec)	Amplitude (pA)	Integration time (msec)	Saturating current (pA)	N
Wild type	65 ± 4	210 ± 11	0.75 ± 0.06	306 ± 20	13.7 ± 0.7	47
H258N	68 ± 5	200 ± 15	1.00 ± 0.12	274 ± 53	12.2 ± 1.9	9